PI-V plus Sliding Mode Based Cascade Control of Magnetic Levitation

Yakup Eroğlu, Günyaz Ablay

Department of Electrical & Electronics Engineering, Abdullah Gül University, Kayseri, Turkey
yakup.eroglu@agu.edu.tr, gunyaz.ablay@agu.edu.tr

Abstract

Magnetic levitation systems are able to provide frictionless, reliable, fast and economical operations in wide-range applications. The effectiveness and applicability of these systems require precise feedback control design. The position control problem of the magnetic levitation can be solved with robust current control approaches. A cascade control approach consisting of PI-velocity plus sliding mode control (PI-V plus SMC) is designed to render high control performance and robustness to the magnetic levitation. It will be shown that the SMC designed for electrical part of the plant (current controller) is able to eliminate the effects of the inductance related uncertainties of the electromagnetic coil of the plant. Experimental results are provided to validate the efficacy of the approach.

1. Introduction

Magnetic levitation technology provides contactless movement and removes friction problem. It has been used in many industrial systems including in high-speed maglev trains, frictionless bearings, electromagnetic cranes, levitation of wind tunnel models, vibration isolation of sensitive machinery, levitation of molten metal in induction furnaces, rocket-guiding projects, levitation of metal slabs during manufacture and high-precision positioning of wafers in photolithography [1]–[8]. This technology is able to serve reliable and high-speed operations with the use of feedback controllers. On the other hand, it is difficult to provide high control performance with standard controllers for the magnetic levitation systems because of their open-loop unstable and highly nonlinear dynamics, and existence of parameter uncertainties due to inductance of the electromagnetic coil.

Recently, many works have been reported for controlling magnetic levitation in the literature. The designed control techniques include feedback linearization based controllers (including input-output and input-state linearization techniques) [4], [6], [9]–[11], linear state feedback control design [6], [12], the gain scheduling approach [13], observer-based control [5], neural network techniques [14], sliding mode controllers [8], [15], [16], backstepping control [17], model predictive control [18] and PID controllers [19]. In short, many known linear and nonlinear control methods were designed for magnetic levitation systems. In the linear controller designs, the approximate linear model found by perturbing the system dynamics about a desired operating point is used, and thus, the controllers are usually valid only around the operating point. The performance of the linear controllers can be improved with some kind of gain scheduling procedure to change operating points, but the stability may not be guaranteed. Since the governing differential equations are highly nonlinear, the nonlinear controllers seem more attractive. However, many nonlinear control designs need exact knowledge about the plant nonlinearities to ensure a good performance. The modeling and parameter uncertainties in the magnetic levitation plant model makes practical implementations of the nonlinear controllers difficult.

In this work, a practical cascade control approach is considered. The cascade control allows us to design a high gain inner loop (current) controller to deal with the effects of plant disturbance and uncertainty. Since the plant is composed of mechanical and electrical parts, the cascade controller can give a good performance. For the mechanical part of the system, a PI plus velocity controller is designed for tracking control of the position of the plant. For the electrical part which is much faster than the mechanical part, a sliding mode controller (SMC) is designed for ensuring high performance current controller. The SMC has ability to render robustness in the presence of inductance uncertainties. The effectiveness of the method is demonstrated with numerical simulations and experimental tests. It is shown that the PI-V plus SMC based cascade controller can provide highly satisfactory tracking performance with a small tracking error for the magnetic levitation system in the existence of coil inductance uncertainty.

This paper is organized as follows: Section 2 provides a background on magnetic levitation system. Controller design strategy is given in Section 3, and application results are given in Section 4. Conclusion of the study is provided in Section 5.

2. Magnetic Levitation and Modeling

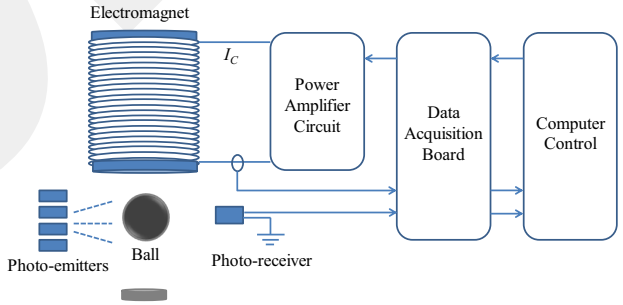

Fig. 1. Schematic diagram of a single-axis magnetic levitation system.

Magnetic levitation system is used to levitate a steel ball in air due to the electromagnetic force created by an electromagnet. The system consists of an electromagnet, a steel ball, a ball post and a ball position sensor. A schematic diagram of the magnetic levitation system used in the experimental studies is shown in Fig. 1. The entire system is encased in a rectangular enclosure which contains three distinct sections. The upper section contains an electromagnet, made of a solenoid coil with a steel core. The middle section consists of a chamber where the ball suspension takes place. One of the electromagnet poles faces the

top of a black post upon which a one inch steel ball rests. A photo sensitive sensor embedded in the post measures the ball elevation from the post. The last section of the system houses the signal conditioning circuitry needed for light intensity position sensor. The ball is only controlled through vertical x-axis. The attraction force is controlled by the computer controlled electromagnet mounted directly above the levitation ball. The photo detector consists of an NPN silicon photodarlington. The electromagnet consists of a tightly wound solenoid coil made of 2450 turns of 20 AWG magnet wire. Electromagnet coil input supply is ±24V with a maximum 3A coil current. The data acquisition board is a successive approximation type, 12-bit analog and digital conversion board capable of 4 kHz sampling. In this work, the controllers are implemented at a sampling rate of 1 kHz. The entire system is decomposed into two subsystems, namely mechanical and electrical subsystems, as seen Fig. 2. The coil current is adjusted to control the ball position in the mechanical system, whereas the coil voltage is varied to control the coil current in the electrical system. Thus, the voltage applied to the electromagnet indirectly controls the ball position. In the following subsections, we obtain the nonlinear mathematical model of the system by using Fig. 2.

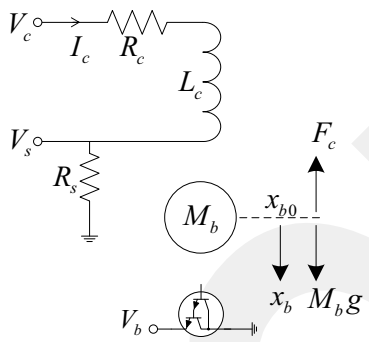

Fig. 2. Dynamical modeling of the magnetic levitation system.

Table 1. Plant parameters

Symbol	Description	Value
L_c	Coil inductance	412.5mH
R_c	Coil resistance	10Ω
R_s	Current sense resistance	1Ω
K_m	Electromagnet force constant	$6.53\text{x}10^{-5}$ Nm^2/A^2
M_b	Steel ball mass	0.068kg
K_B	Position sensor sensitivity	$2.83\text{x}10^{-3}$m/V
N_c	Number of turns in coil wire	2450

2.1. Modeling of the Mechanical Part

Using the notation and conventions given in Fig. 2, the mechanical model of the plant can be obtained. By applying Newton's second law of motion to the ball, the force balance equation of the ball is given with the following second-order model:

$$M_b \ddot{x}_b = M_b g - F_c \tag{1}$$

where x_b is the air gap (in m), M_b is the mass of the ball (in kg), g is the gravitational constant (in m/s^2) and F_c is the force generated by the electromagnet (in N). Attractive force generated by the electromagnet is given by [20]

$$F_c = \frac{K_m}{2}\left(\frac{I_c}{x_b}\right)^2 \tag{2}$$

where K_m is the electromagnet force constant (in Nm^2/A^2) and I_c is the coil current (in A). At equilibrium point, all the time derivatives are set to zero.

$$-\frac{K_m I_c^2}{2M_b x_b^2} + g = 0 \tag{3}$$

From Eq. (3), the coil current at equilibrium position, I_{c0} , can be expressed as a function of x_{b0} and K_m.

$$I_{c0} = \sqrt{\frac{2M_b g}{K_m}}\, x_{b0} \tag{4}$$

The nominal coil current I_{c0} for the electromagnet ball pair can be obtained at the system's static equilibrium. The static equilibrium at a nominal operating point (x_{b0}, I_{c0}) is characterized by the ball being suspended in air at a stationary point x_{b0} due to a constant attractive force created by I_{c0}.

2.2. Modeling of the Electrical Part

By assuming that the coil inductance is constant around the operation point and applying Kirchhoff's voltage law to the electromagnet (RL circuit in Fig. 2), the electrical model of the magnetic levitation can be written as

$$\frac{dI_c}{dt} = -\frac{R_c + R_s}{L_c} I_c + \frac{1}{L_c} V_c \tag{5}$$

where I_c is the coil current, L_c is the coil inductance (in H), R_c is the coil resistance(in Ω), R_s is the current sense resistance (in Ω) and V_c is the supply voltage (in V). The transfer function of the electrical circuit can be obtained by applying Laplace transform to Eq. (5)

$$G_c(s) = \frac{I_c(s)}{V_c(s)} = \frac{K_c}{\tau_c s + 1} \tag{6}$$

where $K_c = \frac{1}{R_c + R_s}$ is the dc gain, and $\tau_c = \frac{L_c}{R_c + R_s}$ is the time constant of the electrical subsystem. In nature, the electrical subsystem is much faster than the mechanical subsystem. All system parameters are given in Table 1.

2.3. Linearization of the Plant Model

In order to analyze the magnetic levitation, the system can be linearized around equilibrium point (x_{b0}, I_{c0}), the point at which the system will converge as time tends to infinity. Applying Taylor series approximation about equilibrium point (x_{b0}, I_{c0}) to Eq.(1), we get

$$\ddot{x}_b = -\frac{K_m I_{c0}^2}{2M_b x_{b0}^2} + g + \frac{K_m I_{c0}^2}{M_b x_{b0}^3} x_b - \frac{K_m I_{c0}}{M_b x_{b0}^2} I_c \tag{7}$$

Substituting Eq. (4) into (7), we get

$$\ddot{x}_b = \frac{2g}{x_{b0}} x_b - \frac{2g}{I_{c0}} I_c \tag{8}$$

Thus, applying Laplace transform in Eq. (8), transfer function of linearized system around the operation point is obtained as

$$G_b(s) = \frac{X_b(s)}{I_c(s)} = -\frac{K_b w_b^2}{s^2 - w_b^2} \tag{9}$$

where $K_b = x_{b0}/I_{c0}$ and $w_b = \sqrt{2g/x_{b0}}$. In this work, it is assumed that the operating point of the system is x_{b0}= 6mm and

I_{c0}= 0.86A. The open-loop transfer function of the system is of type zero and second-order. The two open-loop poles of the system are located at $s = \pm w_b$ which indicates that the open loop system is unstable due to location of poles on the right half of the s-plane. Thus, a feedback controller must be designed to stabilize the system.

3. Controller Design

PI-V plus sliding mode based cascade control is considered to apply the magnetic levitation system. The proposed control scheme is shown in Fig. 3. The PI-V controller will be designed for controlling the outer position loop, while the sliding mode controller will be designed to control the inner coil current. SMC is designed for the electrical part of the system because of its robust and fast response characteristics.

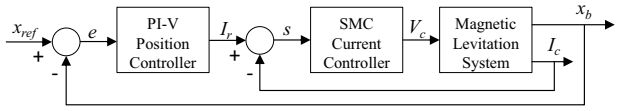

Fig. 3. A cascade control scheme for the magnetic levitation system.

3.1. PI-V Position Controller

The PI-V controller will be designed and tuned with pole placement by using convenient specifications to control the ball position of the mechanical part. In the controller design, the velocity controller is designed to enhance the transient performance and a setpoint weighting is applied to the proportional controller to have a good steady-state response. The objective of the control strategy is to regulate and track the ball position in mid-air. The desired performance requirements are taken as (1) percentage overshoot ≤5%, (2) maximum settling time ≤0.3s, for the position control.

To achieve the desired performance requirements, consider the characteristic equation of third order transfer function

$$(s^2 + 2\zeta\omega_n + \omega_n^2)(s + p_0) = 0 \tag{10}$$

where damping ratio should be ζ=0.69 and natural frequency is found as ω_n=19.3 rad/s. The third pole location is selected as p_0=40 by taking into account the feature [p_0<dominant pole].

Now, the PI-V with set point weighting is designed by

$$I_r(t) = k_p(b_{sp}x_{ref} - x_b) + k_i\int(x_{ref} - x_b)dt + k_v\frac{dx_b(t)}{dt} \tag{11}$$

The Laplace transform of Eq. (11) is

$$I_r(s) = k_p b_{sp}X_{ref}(s) - k_p X_b(s) + \frac{k_i}{s}(X_{ref}(s) - X_b(s)) + k_v s X_b(s) \tag{12}$$

Hence, the closed-loop transfer function can be written as

$$T_b(s) = \frac{X_b(s)}{X_{ref}(s)} = \frac{I_r(s)}{X_{ref}(s)}\frac{V_c(s)}{I_r(s)}G_c(s)G_b(s) \tag{13}$$

with the assumption $I_r(s) = I_c(s)$ due to inner current loop control, namely,

$$\frac{V_c(s)}{I_r(s)}G_c(s) = 1 \tag{14}$$

Thus, the closed loop position transfer function is

$$T_b(s) = \frac{X_b(s)}{X_{ref}(s)} = \frac{I_r(s)}{X_{ref}(s)}G_b(s) \tag{15}$$

Substituting Eq. (12) into Eq. (15), we obtain

$$T_b(s) = \frac{2gx_{b0}(k_p s + k_i + k_p s(b_{sp} - 1))}{-I_{c0}x_{b0}s^3 + 2gx_{b0}k_v s^2 + 2g(x_{b0}k_p + I_{c0})s + 2gx_{b0}k_i} \tag{16}$$

Controller gains can be obtained by comparing the characteristic equation of closed-loop system (16) with the desired characteristic equation (10). Three separate gains are used in PI-V controller design. The objective of set pointing action is to compensate for the gravitational bias. When the PI-V controller compensates for dynamic disturbances around the linear operating point (x_{b0}, I_{c0}), the setpoint weighting eliminates the changes in the force created due to gravitational bias.

3.2. Sliding Mode Current Controller

Sliding mode controller is considered to control the coil current due to its fast response and robustness features. Since the coil inductance is a function of ball position, but it is taken as constant to simplify analysis and designs, there exists a parameter uncertainty. The effects of inductance related uncertainties can be minimized by designing a high-gain SMC for controlling electrical part of the system current.

To design SMC, first a sliding surface, *s,* can be designed as

$$s = I_r - I_c \tag{17}$$

Thus, the time-derivative of (17), $\dot{s}$, is obtained as

$$\dot{s} = \dot{I}_r + \frac{R_c + R_s}{L_c}I_c - \frac{1}{L_c}V_c \tag{18}$$

To achieve a sliding mode, i.e., $s = \dot{s} = 0$, the voltage V_c as the control input of the magnetic levitation can be designed as [21], [22]

$$V_c = \alpha|s|^{0.5}\,\mathrm{sat}(s) + \beta\int|s|^{0.5}\,\mathrm{sat}(s)dt \tag{19}$$

where

$$\mathrm{sat}(s) = \begin{cases} \mathrm{sgn}(s), & if \quad |s| \geq \varepsilon \\ s/\varepsilon\ , & if \quad |s| < \varepsilon \end{cases} \tag{20}$$

The saturation function, sat(.), is used to eliminate chattering on the system output. The stability of the SMC (or reachability condition $s\dot{s} < 0$) must be satisfied for selected appropriate gains, α and β. A detailed Lyapunov based stability and robustness analysis can be found in our previous studies (see [21], [22]). Since a boundary layer approach (sat(.) function) is used in the controller design, the trajectory reaches a small ultimate bound set in finite time. This means that the tracking error stays around the origin, but usually not in the origin. The appropriate gain values can be obtained via simulation.

4. Results

The experimental hardware-in-the-loop (HIL) test and numerical simulation results of the proposed cascade control scheme for the magnetic levitation are provided in this section. In both numerical and experimental studies, MATLAB/Simulink programs are used. The control parameters are obtained based on desired performance requirements and verified with numerical simulations as k_p=-199.7, k_i=-633.2, k_v=-2.82 and b_{sp}=0.35 for PI-V controller with set-point weighting, and α=150 and β=50 for the SMC.

4.1. Numerical Simulations

In numerical simulations, it is assumed that the ball position varies from 8 to 10 mm ramp signals with a frequency of 0.25Hz. From the desired performance requirements (see Section 3.1), the controller should accomplish a desired ± 1mm square wave position set point.

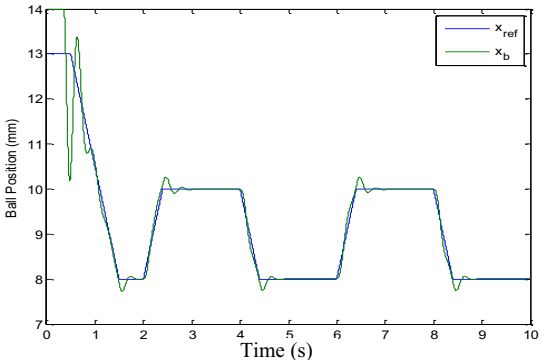

Fig. 4. Ball position trajectory

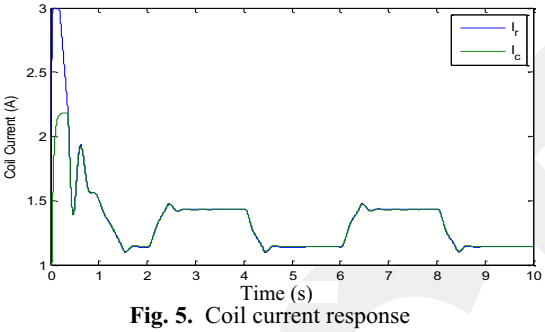

Fig. 5. Coil current response

The tracking performance of the cascade PI-V plus SMC controller is illustrated in Figs. 4-8. It is seen in Fig. 4 that the controller provides a desired tracking performance with a little overshoot (around 2%). Figure 5 shows the response of the SMC current controller in which the coil current perfectly tracks the desired current, which makes the ball to follow the reference trajectory. The control signal, i.e., coil voltage, is shown in Fig. 6. Smooth voltage and current signals are observed in the simulations. The tracking error, which is the difference between actual trajectory and reference trajectory, is shown in Fig. 7. The tracking error has little short transient response which satisfies the required settling time, and about 0.2mm (2% overshoot) in simulations. Fig. 8 shows that the sliding surface, *s*, goes to zero in a short time and stays around zero for all subsequent times.

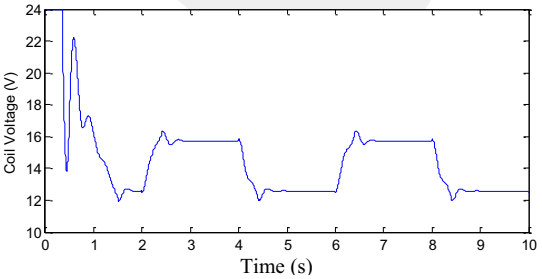

Fig. 6. Coil voltage response

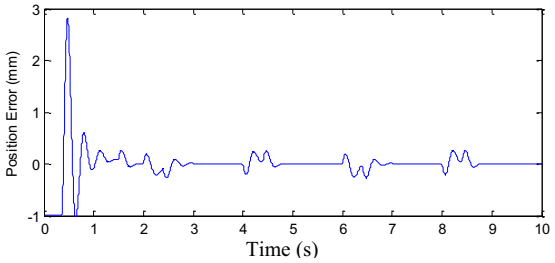

Fig. 7. Position tracking error

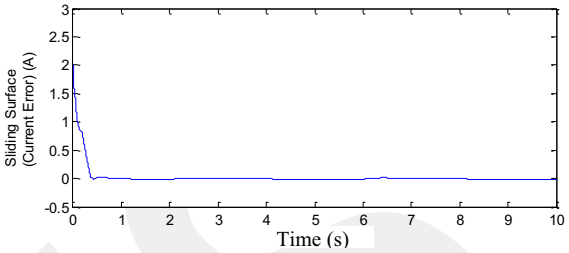

Fig. 8. Current tracking error

4.2. Experimental Results

To compare the numerical and experimental results, the similar position reference is applied. The experimental results are shown in Figs. 9-13. Figure 9 shows that the controller holds the ball during startup and follows the reference position trajectory thereafter. The small oscillations around the reference point are due to the effects of sampling, measurement error and noise. In addition, the ball sways right and left rather than staying vertically as the photo detector cannot exactly measure the ball position because of circularity of the ball. This can be solved with touching lightly to the ball by hand. In 6th second we touched the ball around 0.5 seconds to center the ball, and after that point, it can be seen that the tracking results are improved.

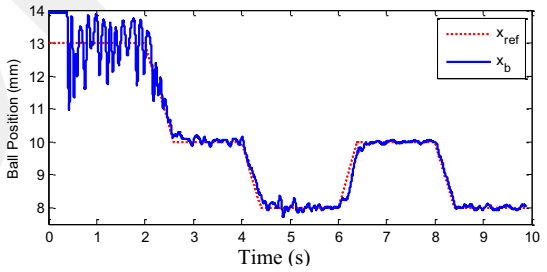

Fig. 9. Experimental ball position trajectory

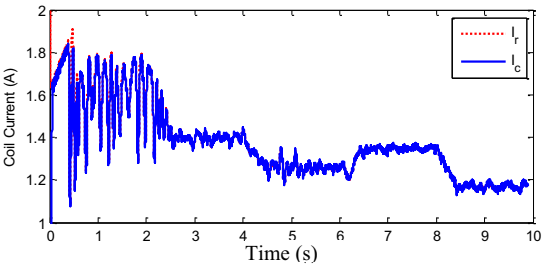

Fig. 10. Experimental coil current response

Figure 10 shows the response of the coil current. The SMC current controller eliminates the effects of inductance uncertainty and provides a highly satisfactory tracking

performance. The response of the coil voltage is shown in Fig. 11. The average voltage supply is around 14V during steady-state. The position tracking error is shown in Fig. 12. It is clear that the position error is limited about 0.2mm during steady-state which satisfies desired requirements. The position error is decreased to 0.1mm after the light touch to the ball by hand. Figure 13 shows the sliding surface, *s*, (or current tracking error). It is seen that the sliding surface reaches zero in a short time and stays around zero thereafter.

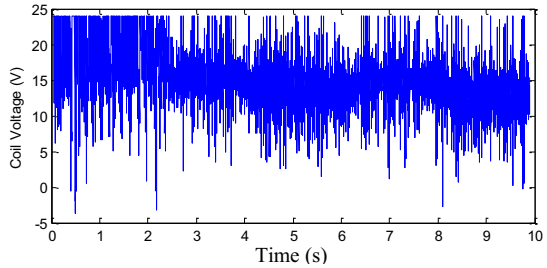

Fig. 11. Experimental coil voltage response

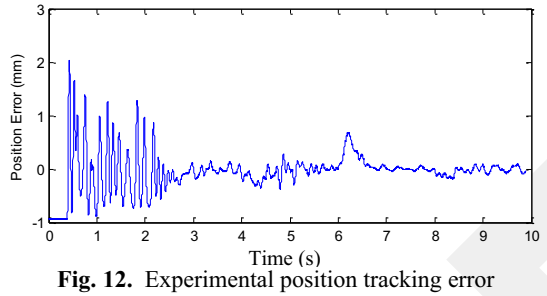

Fig. 12. Experimental position tracking error

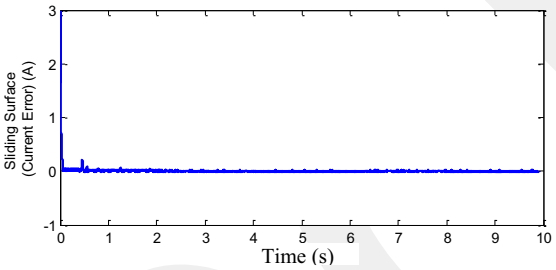

Fig. 13. Experimental current tracking error

5. Conclusion

A PI-V plus SMC based cascade controller is designed for feedback control of the magnetic levitation. Both numerical simulation and experimental test results are given to demonstrate the effectiveness of the controller. A high gain SMC is designed for current control of the magnetic levitation system in order to eliminate coil inductance originated disturbance and uncertainty. The results show that the method provides a highly satisfactory tracking control performance in the presence of coil inductance uncertainty.

6. Acknowledgement

This work was supported by Turkish Scientific and Research Council (TUBITAK) under project number 113E329.

7. References

[1] Y. Luguang, "Progress of the Maglev Transportation in China," *IEEE Transactions on Applied Superconductivity*, vol. 16, no. 2, pp. 1138–1141, Jun. 2006.

[2] D. F. Berdy, D. J. Valentino, and D. Peroulis, "Kinetic energy harvesting from human walking and running using a magnetic levitation energy harvester," *Sensors and Actuators A: Physical*, vol. 222, pp. 262–271, Feb. 2015.

[3] K. Ozturk, E. Sahin, M. Abdioglu, M. Kabaer, S. Celik, E. Yanmaz, and T. Kucukomeroglu, "Comparative study of the magnetic stiffness, levitation and guidance force properties of single and multi seeded YBCOs for different HTS–PMG arrangements," *Journal of Alloys and Compounds*, vol. 643, pp. 201–206, Sep. 2015.

[4] A. El Hajjaji and M. Ouladsine, "Modeling and nonlinear control of magnetic levitation systems," *IEEE Transactions on Industrial Electronics*, vol. 48, no. 4, pp. 831–838, Aug. 2001.

[5] U. Hasirci, A. Balikci, Z. Zabar, and L. Birenbaum, "A Novel Magnetic-Levitation System: Design, Implementation, and Nonlinear Control," *IEEE Transactions on Plasma Science*, vol. 39, no. 1, pp. 492–497, Jan. 2011.

[6] W. Barie and J. Chiasson, "Linear and nonlinear state-space controllers for magnetic levitation," *International Journal of Systems Science*, vol. 27, no. 11, pp. 1153–1163, Nov. 1996.

[7] S. Yamamura and H. Yamaguchi, "Electromagnetic levitation system by means of salient-pole type magnets coupled with laminated slotless rails," *IEEE Transactions on Vehicular Technology*, vol. 39, no. 1, pp. 83–87, 1990.

[8] D. Cho, Y. Kato, and D. Spilman, "Sliding mode and classical controllers in magnetic levitation systems," *IEEE Control Systems*, vol. 13, no. 1, pp. 42–48, Feb. 1993.

[9] F. Beltran-Carbajal, A. Valderrabano-Gonzalez, J. C. Rosas-Caro, and A. Favela-Contreras, "Output feedback control of a mechanical system using magnetic levitation," *ISA Transactions*, vol. 57, pp. 352–359, Jul. 2015.

[10] R. Morales and H. Sira-Ramírez, "Trajectory tracking for the magnetic ball levitation system via exact feedforward linearisation and GPI control," *International Journal of Control*, vol. 83, no. 6, pp. 1155–1166, Jun. 2010.

[11] C. Nielsen, C. Fulford, and M. Maggiore, "Path following using transverse feedback linearization: Application to a maglev positioning system," in *American Control Conference, 2009. ACC '09.*, 2009, pp. 3045–3050.

[12] O. M. El Rifai and K. Youcef-Toumi, "Achievable performance and design trade-offs in magnetic levitation control," in *, 1998 5th International Workshop on Advanced Motion Control, 1998. AMC '98-Coimbra*, 1998, pp. 586–591.

[13] Y. C. Kim and K.-H. Kim, "Gain scheduled control of magnetic suspension system," in *American Control Conference, 1994*, 1994, vol. 3, pp. 3127–3131 vol.3.

[14] S.-Y. Chen, F.-J. Lin, and K.-K. Shyu, "Direct decentralized neural control for nonlinear MIMO magnetic levitation system," *Neurocomputing*, vol. 72, no. 13–15, pp. 3220–3230, Aug. 2009.

[15] N. F. Al-Muthairi and M. Zribi, "Sliding mode control of a magnetic levitation system," *Mathematical Problems in Engineering*, vol. 2004, no. 2, pp. 93–107, 2004.

[16] F.-J. Lin, S.-Y. Chen, and K.-K. Shyu, "Robust Dynamic Sliding-Mode Control Using Adaptive RENN for Magnetic Levitation System," *IEEE Transactions on Neural Networks*, vol. 20, no. 6, pp. 938–951, Jun. 2009.

[17] F.-J. Lin, L.-T. Teng, and P.-H. Shieh, "Intelligent Adaptive Backstepping Control System for Magnetic Levitation Apparatus," *IEEE Transactions on Magnetics*, vol. 43, no. 5, pp. 2009–2018, May 2007.

[18] T. Bächle, S. Hentzelt, and K. Graichen, "Nonlinear model predictive control of a magnetic levitation system," *Control Engineering Practice*, vol. 21, no. 9, pp. 1250–1258, Sep. 2013.

[19] E. V. Kumar and J. Jerome, "LQR based Optimal Tuning of PID Controller for Trajectory Tracking of Magnetic Levitation System," *Procedia Engineering*, vol. 64, pp. 254–264, 2013.

[20] B. V. Jayawant and D. P. Rea, "New electromagnetic suspension and its stabilisation," *Proceedings of the Institution of Electrical Engineers*, vol. 115, no. 4, pp. 549–554, Apr. 1968.

[21] G. Ablay, "Variable structure controllers for unstable processes," *Journal of Process Control*, vol. 32, pp. 10–15, Aug. 2015.

[22] G. Ablay and Y. Eroglu, "Variable structure controllers for processes," in *Turkish Automatic Control Conference, TOK2015*, Denizli, 2015.